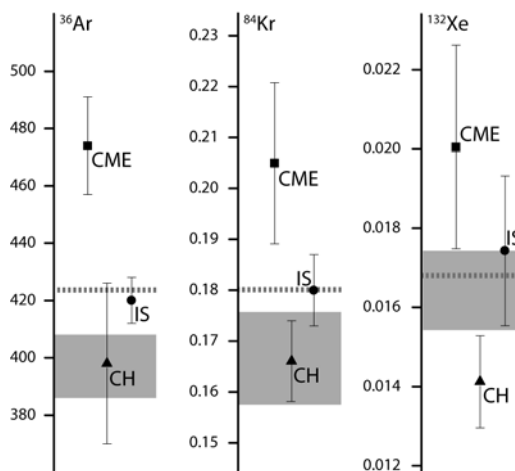


**ARGON, KRYPTON, AND XENON IN THREE SOLAR WIND REGIMES AS COLLECTED BY GENESIS** N. Vogel<sup>1</sup>, H. Baur<sup>1</sup>, D.S. Burnett<sup>2</sup>, C. Maden<sup>1</sup>, and R. Wieler<sup>1</sup>. <sup>1</sup>Institute for Geochemistry and Petrology, ETH Zurich, Switzerland. nadia.vogel@erdw.ethz.ch. <sup>2</sup>CalTech, JPL, Pasadena, USA.

**Introduction:** The goal of the GENESIS mission was not only to determine the bulk solar wind (SW) composition, but also the composition of the individual SW “regimes” [1]. These are the slow interstream (IS) wind, the fast (CH) wind originating in large coronal holes, and SW related to coronal mass ejections (CMEs), which originate in magnetically active regions on the Sun [2]. To collect regime-related SW, separate collector arrays were deployed according to an on-board algorithm taking into account parameters like the SW proton speed and temperature, abundance of alpha particles, and the angular distribution of suprathermal electrons [3, 4]. Regime targets collected slow, fast, and CME-related SW for 334, 313, and 193 days, respectively [2]. Light noble gas regime data were presented and discussed by [5, 6]: CME-related SW showed a distinctive light element enrichment compared to the CH, and IS SW. Also, the regimes showed significant differences in their He isotopic compositions, smaller ones for Ne, and hardly discernible ones for Ar. We therefore assume that Kr and Xe do not show measurable isotope fractionation, and focus on analyzing the elemental composition (<sup>36</sup>Ar, <sup>84</sup>Kr, <sup>132</sup>Xe) of the regime targets instead. The data will be compared to those measured in the bulk SW [8, 9] and to each other in order to rule on potential element fractionation during solar wind formation. This will ultimately help to infer the photospheric (i.e. solar) heavy noble gas composition from that of the SW.

**Experimental:** We analyzed <sup>36</sup>Ar, <sup>84</sup>Kr, and <sup>132</sup>Xe extracted from 20–40 mm<sup>2</sup> of Czochralski (CZ)-grown Si targets [10] by UV laser ablation. The analytical techniques are described in detail by [9]. In order to verify quantitative gas release, a re-extraction was performed on each ablated area. With one exception, gas concentrations of the re-extractions never exceeded those determined on non-flown but otherwise identical pieces of CZ-Si (material blanks). We point out that the material blanks analyzed so far are quite variable in Kr and Xe, and more measurements are necessary to better constrain the Kr and Xe concentrations indigenous to the target material. Total blank contributions (i.e. from procedural and material blanks) to measured sample gas concentrations were negligible for <sup>36</sup>Ar and below ~3% and ~10% for <sup>84</sup>Kr and <sup>132</sup>Xe, respectively. Due to the low Kr and Xe amounts in samples, re-extractions, and material blanks, data regression is not trivial. Besides counting statistics the blank correction often represents a major source of uncertainty.

**Results:** All results presented here are preliminary. Averages for each SW regime are calculated from 5–6 individual analyses, error bars reflect the scatter of the data. Fig. 1 shows that the Ar, Kr, and Xe fluxes are significantly higher in the CME-related SW than in the fast (CH) and slow (IS) wind. It further seems that the Ar, Kr, and Xe fluxes in the slow SW are somewhat higher than in the fast SW, although hardly outside 1 $\sigma$  uncertainties. Using the relative exposure times of the different SW regimes (CME ~22%, IS ~40%, CH ~38%; [2]), we calculated “theoretical bulk SW fluxes” (Fig. 1, dashed lines). Note that these have substantial uncertainties, which are not shown in the plot. Taking into account these uncertainties, all theoretical bulk SW fluxes agree well with the respective measured bulk SW fluxes (Fig. 1, grey boxes).



**Fig. 1:** Average <sup>36</sup>Ar, <sup>84</sup>Kr, and <sup>132</sup>Xe fluxes in atoms/(cm<sup>2</sup>\*s) in the fast (CH, triangle), slow (IS, circle), and CME-related (CME, square) SW. Uncertainties are 1 $\sigma$  standard deviations of averages. Grey boxes represent measured bulk SW fluxes [9]; dashed lines indicate calculated theoretical bulk SW fluxes using regime target exposure times given by [2].

Fig. 2 shows the element ratios <sup>36</sup>Ar/<sup>84</sup>Kr and <sup>84</sup>Kr/<sup>132</sup>Xe averaged from the individual measurements of the respective regime targets. The <sup>36</sup>Ar/<sup>84</sup>Kr ratios of slow, fast, and CME-related SW are identical within uncertainties to each other and to the measured and theoretical bulk solar wind ratios. In contrast, the average <sup>84</sup>Kr/<sup>132</sup>Xe ratio of the fast SW is significantly higher than those of the slow and CME-related SW, which in turn are identical to each other.

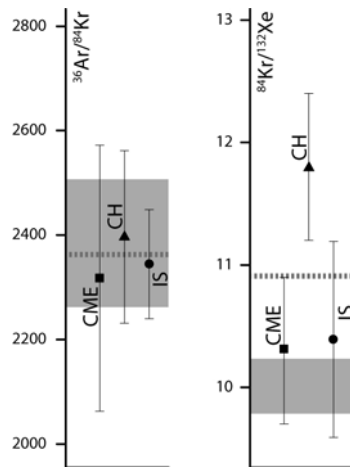


**Fig. 2:** Average element ratios  $^{36}\text{Ar}/^{84}\text{Kr}$  and  $^{84}\text{Kr}/^{132}\text{Xe}$  in the fast (CH, triangle), slow (IS, circle), and CME-related (CME, square). See figure caption of Fig. 1 for further information.

**Discussion:** Despite the challenging analyses with sample gas amounts not much above blank and sensitivity limits, the preliminary heavy noble gas regime data provide some robust new results. The  $^{36}\text{Ar}$ ,  $^{84}\text{Kr}$ , and  $^{132}\text{Xe}$  fluxes in the CME-related SW are on average ~20% higher than those in the fast and slow SW. Note that also the He flux of the CME-related SW is ~20% higher than the He fluxes of the fast and the slow SW [11]. The  $^{36}\text{Ar}/^{84}\text{Kr}$  ratios are within uncertainties identical in all different SW regimes; i.e. the degree of fractionation of Ar and Kr from photospheric composition is identical in all three SW regimes, although the different SW types originate in different regions on the Sun and have different velocities. This result contrasts with that of [5] who found a pronounced enrichment of He and Ne relative to Ar in CME-related SW compared to the slow and fast SW. In contrast to the uniform  $^{36}\text{Ar}/^{84}\text{Kr}$  ratios, the  $^{84}\text{Kr}/^{132}\text{Xe}$  ratio of the fast SW is significantly higher than those of the slow and CME-related SW. It is assumed that the fast SW is elementally less fractionated than the slow and the CME-related SW compared to the photosphere [e.g., 6, 12]. Indeed, the  $^{84}\text{Kr}/^{132}\text{Xe}$  ratio of the fast SW is closest to the photospheric  $^{84}\text{Kr}/^{132}\text{Xe}$  ratio with a value of ~20 [13, 14]. [15, 16] proposed a secular change of the bulk SW  $^{84}\text{Kr}/^{132}\text{Xe}$  ratio based on lunar regolith grains of different antiquity, while the  $^{36}\text{Ar}/^{84}\text{Kr}$  ratio remained constant. The underlying mechanism(s) for this specific SW evolution are unclear. Different proportions of fast SW contributing to the total SW flux at different times in the past might help to explain the observation made by [15, 16]. Fig. 3 shows the fractionation of the heavy noble gases normalized to O in the different SW regimes relative to the photosphere as a function of the

first ionization potentials (FIP) of the elements. The high-FIP elements Ar and Kr are uniformly depleted in all SW regimes relative to the photosphere. Thus, the Ar/Kr ratios in all SW regimes reflect within uncertainties photospheric, i.e. solar composition. Xe in all SW regimes is within uncertainties unfractionated or possibly slightly enriched relative to the photosphere and O. These results agree well with those deduced from the comparison of bulk SW noble gas data with photospheric values [7, 9].

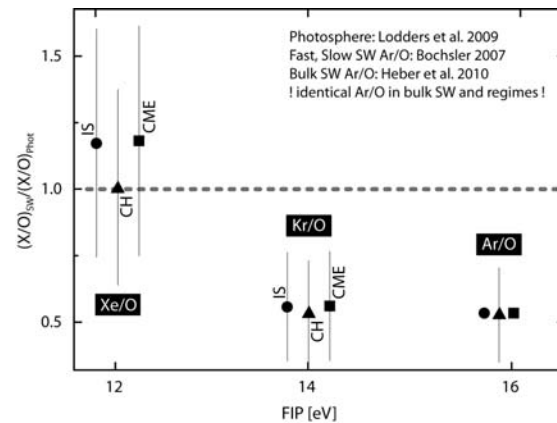


**Fig. 3:** Element fractionation in the fast (CH), slow (IS), and CME-related SW compared to photospheric composition [14] as a function of FIP. For better visibility CH ratios plot on the correct FIP, while IS and CME ratios are slightly shifted. SW Ar/O ratios: [17, 18].

**Acknowledgements:** We thank the Genesis Sample Curation Team and the Swiss National Science Foundation for their support.

**References:** [1] Burnett D.S., et al. (2003) *Space Science Reviews*, 105, 509-534. [2] Reisenfeld D.B., et al. (2007) *Space Science Reviews*, 130, 79-86. [3] Barraclough B.L., et al. (2003) *Space Science Reviews*, 105, 627-660. [4] Neugebauer M., et al. (2003) *Space Science Reviews*, 105, 661-679. [5] Heber V.S., et al. (2008) *LPSC*, 39, A1778. [6] Heber V.S., et al. (2009) *LPSC*, 40, A2503. [7] Vogel N., et al. (2010) *LPSC*, 41, A1893. [8] Heber V.S., et al. (2009) *Geochimica et Cosmochimica Acta*, 73, 7414-7432. [9] Vogel N., et al. *submitted to Geochimica et Cosmochimica Acta* [10] Jurewicz A.J.G., et al. (2003) *Space Science Reviews*, 105, 535-560. [11] Wiens R.C., et al. (2006) *Report to NASA Genesis Mission Science Team*, 1-33. [12] Wiens R.C., et al. (2010) *LPSC*, 41, A2125. [13] Asplund M., et al. (2009) *Annual Review of Astronomy and Astrophysics*, 47, 481-522. [14] Lodders K., et al., *Abundances of the elements in the solar system*, in *SpringerMaterials - The Landolt-Börnstein Database*, J.E. Trümper, Editor. 2009, Springer Verlag Berlin Heidelberg: Berlin. p. 1-59. [15] Wieler R. and Baur H. (1995) *The Astrophysical Journal*, 453, 987-997. [16] Wieler R., et al. (1996) *Nature*, 384, 46-49. [17] Bochsler P. (2007) *The Astronomy and Astrophysics Review*, 14, 1-40. [18] Heber V.S., et al. (2010) *LPSC*, 41, A2234.